Catalysis Communications 46 (2014) 98–102

Contents lists available at ScienceDirect

Catalysis Communications

journal homepage: www.elsevier.com/locate/catcom

Short Communication

Basic oxide-supported Ru catalysts for liquid phase glycerol hydrogenolysis in an additive-free system

Jian Feng [a,*], Wei Xiong [a], Bin Xu [b], Weidong Jiang [b], Jinbo Wang [a], Hua Chen [c]

[a] College of Chemistry and Chemical Engineering, Chongqing University of Science & Technology, Chongqing 401331, China
[b] Key Laboratory of Green Catalysis of Sichuan Institutes of Higher Education, School of Chemistry and Pharmaceutical Engineering, Sichuan University of Science & Engineering, Zigong 643000, China
[c] Key Laboratory of Green Chemistry and Technology, Ministry of Education, College of Chemistry, Sichuan University, Chengdu 610064, China

ARTICLE INFO

Article history:
Received 1 October 2013
Received in revised form 25 November 2013
Accepted 29 November 2013
Available online 7 December 2013

Keywords:
Ruthenium
Basic oxide support
Hydrogenolysis
Glycerol
1,2-Propanediol
Lactic acid

ABSTRACT

Several basic oxide-supported Ru catalysts (Ru/CeO_2, Ru/La_2O_3 and Ru/MgO) were prepared and evaluated for the hydrogenolysis of glycerol. The Ru catalysts were characterized by inductively coupled plasma–atomic emission spectroscopy, nitrogen adsorption, powder X-ray diffraction, X-ray photoelectron spectroscopy, and transmission electron microscopy. Ru/CeO_2 showed the best performance in the reaction, which is associated with its smaller metal particle size and the weak surface basicity feature of CeO_2. 1,2-Propanediol is obtained as the main product through a dehydrogenation–dehydration–hydrogenation mechanism. The oxidation product lactic acid can be formed by a Cannizzaro reaction from the pyruvaldehyde intermediate.

1. Introduction

In recent years, because of the rapid development of biodiesel production by transesterification of vegetable oils or animal fats, large amounts of glycerol are available as a byproduct. How to utilize these biomass-derived glycerol has attracted great attention. In particular, the catalytic hydrogenolysis process is one of the most promising routes in the chemical transformation of glycerol. The main product arising from the hydrogenolysis of glycerol is 1,2-propanediol (1,2-PDO), which is extensively used as a monomer for the production of polyester resins. Undoubtedly, the production of 1,2-PDO from glycerol will be a sustainable and feasible alternative to the current petroleum-based 1,2-PDO production method.

In general, the hydrogenolysis of glycerol is studied under heterogeneous conditions over various metal catalysts. Several recent reviews have summarized relevant catalytic systems for the glycerol hydrogenolysis reaction [1–3]. In order to obtain a good catalytic performance, metal catalysts are usually used in combination with a certain acid or base additive [2,3]. For example, H_2WO_4 [4], cation-exchange resin [5–7] and Nb_2O_5 [8] are effective acid additives, which can enhance the reaction rate and the diol selectivity over Ru or Rh catalysts. Regarding the base additives, Wang and Liu [9] and Maris et al. [10,11] found that the addition of NaOH markedly increased the reactivity of Cu, Ru or Pt catalysts, but a certain amount of lactic acid was formed at high pH. In our previous works [12–16], we have developed a series of Ru-based catalysts, which exhibited good performances in the hydrogenolysis of glycerol to 1,2-PDO. Using LiOH as additive, both the conversion of glycerol and the selectivity to 1,2-PDO can be high up to 90% in the presence of Ru/TiO_2 catalyst [12–14]. We have also demonstrated that the base aids the initial dehydrogenation of glycerol to glyceraldehyde and promotes the dehydration of glyceraldehyde to 2-hydroxyacrolein (see Scheme 1) [12]. This effect of the base additive is responsible for the enhancement in the reaction rate and 1,2-PDO selectivity.

Although the introduction of some additives can promote the catalytic performance, it results in many troubles in practical manipulation, such as the product separation and catalyst recycling. According to the reaction pathway in Scheme 1, a catalyst that contains both metal sites and base sites should also achieve good results in the glycerol hydrogenolysis reaction. Solid-base supported metal catalysts will make it possible for the successful combination of metal sites and base sites. Such metal–base bifunctional catalysts bring the advantage that the product separation or catalyst recycling will be more maneuverable and more practicable. In fact, solid-base supported Pt catalysts [17] and Cu catalysts [18–21] are indeed efficient for the selective hydrogenolysis of glycerol to 1,2-PDO. As a typical example, the research group of Hou [18–20] developed a series of Cu-based catalysts supported on the

---

* Corresponding author. Tel.: +86 23 65023739; fax: +86 23 65023753.
E-mail address: fengjianscu@163.com (J. Feng).

1566-7367/$ – see front matter © 2013 Elsevier B.V. All rights reserved.
http://dx.doi.org/10.1016/j.catcom.2013.11.031

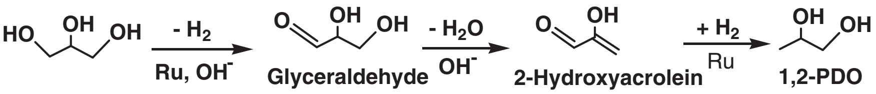

Scheme 1. Hydrogenolysis of glycerol to 1,2-PDO over Ru-based catalyst in basic aqueous solution.

layered double hydrotalcite-like compounds. These Cu-based catalysts were highly selective for 1,2-PDO. However, the catalyst preparation procedure seems a bit complicated and unmanageable.

In this work, we directly utilize the surface basicity of several easily available supports to modify the Ru catalyst, with the intent of developing a simple and additive-free catalytic system. Several Ru catalysts supported on basic oxides (CeO_2, La_2O_3 and MgO) were prepared and examined for the glycerol hydrogenolysis reaction. Ru/CeO_2 was found to be an efficient catalyst for the hydrogenolysis of glycerol in an additive-free aqueous solution.

2. Experimental

2.1. Catalyst preparation

Ru catalysts (Ru/CeO_2, Ru/La_2O_3 and Ru/MgO) with a metal loading of 3 wt.% were prepared by impregnation technique. Weighed amounts of the corresponding oxide were impregnated with the aqueous solution of $RuCl_3$. After impregnation, the solvent was removed, and the resulting powder was dried in vacuum at 110 °C for 10 h. All the catalysts were reduced in an autoclave by hydrogen at 200 °C. For more details, see the Supplementary material.

2.2. Characterizations

The Ru catalysts were characterized by ICP-AES, BET, XRD, XPS, and TEM. According to the references [22,23], the surface basicity features of the oxide supports were determined by the benzoic acid titration method using two Hammett indicators: bromothymol blue ($pKa = +7.2$) and 2,4-dinitroaniline ($pKa = +15.0$). The base strength ($H\_$) was expressed by the Hammett function that was scaled by the pKa values of the indicators. The details are discussed in the Supplementary material.

2.3. Catalytic performance testing

Hydrogenolysis of glycerol was carried out in a 30 mL stainless steel autoclave. Because of the word count limit, more details are presented in the Supplementary material.

3. Results and discussion

3.1. Characterization of catalysts and supports

Some characterization results are shown comparatively in Table 1. ICP-AES results show that the Ru weight loadings are near to the stated value, i.e., about 3 wt.%. The BET surface area of Ru/MgO is the highest, while that of Ru/La_2O_3 and Ru/CeO_2 is very close. The Ru particle sizes are all determined by TEM due to weak diffraction peaks of Ru in the XRD patterns. Obviously, Ru particles are smaller on MgO and CeO_2 than those on La_2O_3. Our previous studies [13,14] have shown that the support material can significantly influence the metal particle size. The bigger Ru particles on La_2O_3 may be related to the fact that Ru particles are easier to agglomerate in this support.

Table 1
Some characterization results of the Ru catalysts.

Catalyst	Ru loading (wt.%)	BET surface area (m^2/g)	Ru particle size (nm)[a]	$Ru^0/(Ru^0 + Ru^{\delta+})$ (%)
Ru/La_2O_3	3.11	59	11.4	100
Ru/MgO	2.98	246	5.8	57.1
Ru/CeO_2	3.03	63	5.3	100

[a] Determined by TEM.

As presented in Table 1, the $Ru^0/(Ru^0 + Ru^{\delta+})$ refers to the surface Ru atomic ratios obtained from XPS experiments, where Ru^0 represents the Ru atoms with metallic state and $Ru^{\delta+}$ represents the Ru species with intermediate value between Ru^0 and Ru^{3+}. The calculation method is referred to our earlier work [13]. It can be seen from Table 1 that the Ru species on Ru/La_2O_3 and Ru/CeO_2 are completely reduced in the reduction process. This indicates that the rare earth element is beneficial to the reduction of Ru, which is in agreement with the findings of Yu and co-workers [24]. A typical Ru 3d XPS spectrum of Ru/CeO_2 is shown in Fig. 1. The singlet in dotted line is attributed to C 1s (binding energy = 284.9 eV). This is an unavoidable contamination signal of the spectrometer [13]. There is only one doublet of Ru 3d (binding energy: Ru $3d_{5/2}$ = 280.1 eV, Ru $3d_{3/2}$ = 284.3 eV), which is assigned to the metallic ruthenium. For reference, the Ru 3d XPS spectra of Ru/MgO and Ru/La_2O_3 are shown in Figs. S1 and S2 (Supplementary material), respectively.

The XRD patterns of the supported Ru catalysts are illustrated in Fig. 2. The crystalline phases were identified by comparison with JCPDS files. For Ru/CeO_2, the clear diffraction peaks at $2\theta = 28.6°$, 33.1°, 47.5°, 56.4°, 59.1°, 69.4°, 76.7°, 79.1° and 88.4° are all attributed to cerianite CeO_2 (JCPDS Card #34-0394). In the case of Ru/MgO, the intensive and sharp diffraction peaks at $2\theta = 18.6°$, 32.8°, 38.0°, 50.8°, 58.6°, 62.1°, 68.2°, 72.0° and 81.2° can be assigned to brucite $Mg(OH)_2$ (JCPDS Card #83-0114), indicating that MgO is converted to $Mg(OH)_2$. This hydration of MgO mainly results from the hydrothermal condition used in the catalyst preparation process [25]. In the XRD pattern of Ru/La_2O_3, a new phase of $La(OH)_3$ ($2\theta = 15.7°$, 27.4°, 31.6° and 48.4°; JCPDS Card #75-1900) is observed accompanied with the phase of La_2O_3 ($2\theta = 27.9°$, 39.6° and 49.5°; JCPDS Card #89-4016). The existence of $La(OH)_3$ could be also owing to the hydrothermal condition in the catalyst preparation process [26]. Accordingly, CeO_2 is comparatively stable under the condition we used. As far as the Ru crystalline phase is concerned, no obvious diffraction peaks can be observed in the XRD patterns of Ru/CeO_2 and Ru/MgO, suggesting that the Ru particles on CeO_2 and MgO are too small to be detected. In contrast, the diffraction peaks of metallic Ru at $2\theta = 38.4°$ and 42.2° (JCPDS Card #89-3942) appeared in the Ru/La_2O_3 catalyst. The particle size of Ru is determined

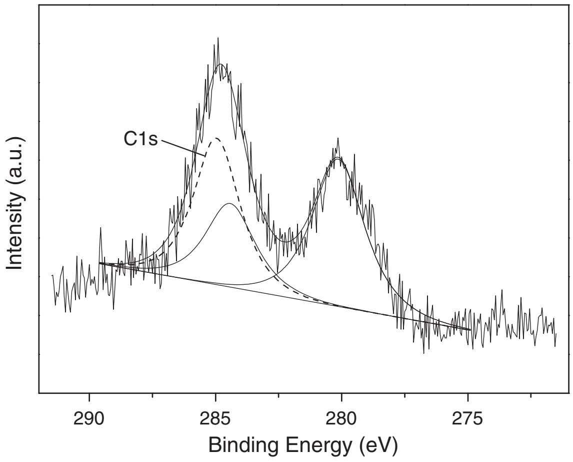

Fig. 1. Ru 3d XPS spectrum of Ru/CeO_2 catalyst.

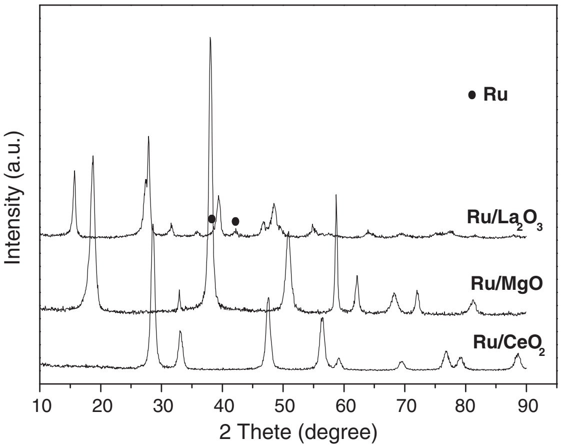

Fig. 2. XRD patterns of the Ru catalysts.

to be about 11.7 nm, which is in accordance with the TEM result listed in Table 1.

The TEM images of the as-prepared Ru catalysts are shown in Fig. 3. The nanosized Ru particles are well dispersed on the surface of CeO_2 and MgO (Fig. 3a and b), giving an average particle size of Ru around 5.5 nm (Table 1). As for the Ru/La_2O_3 catalyst, the dispersion of Ru is not very good (Fig. 3c), and the average particle size of Ru is determined to be about 11.4 nm (Table 1).

As mentioned above, we envisage using the oxide supports to provide base sites. Therefore, the surface basicity features of CeO_2, La_2O_3 and MgO were determined by the benzoic acid titration method as described in the Experimental section. Table 2 presents the base strength distribution of the supports. The base sites between the pKa values of + 7.2 and + 15.0 can be considered as weak base sites [22], whereas those higher than + 15.0 can be assigned as strong base sites [22,23]. Obviously, MgO is a strong base, while CeO_2 and La_2O_3 are weak bases. In addition, there are no strong base sites on the surface of CeO_2.

Table 2
Base strength (H_) distribution of the supports.

Support	Basicity (mmol/g)		
	$+7.2 \leq H\_ \leq +15.0$	$H\_ \geq +15.0$	Total
La_2O_3	0.04	0.01	0.05
MgO	0.08	0.35	0.43
CeO_2	0.13	–	0.13

3.2. Catalytic performance of the Ru catalysts

Catalytic performance results of the Ru/CeO_2, Ru/La_2O_3 and Ru/MgO catalysts in the glycerol hydrogenolysis reaction are presented in Table 3. All the basic oxide-supported Ru catalysts were efficient for the hydrogenolysis of glycerol to 1,2-PDO, ethylene glycol, lactic acid, and monohydroxy-alcohols. The Ru/CeO_2 catalyst exhibited markedly high activity and high selectivity to 1,2-PDO, giving the highest yield of 1,2-PDO (53.4%). In contrast, Ru/La_2O_3 showed the lowest activity, which was about a third of the activity of Ru/CeO_2. Moderate catalytic activity was observed on the Ru/MgO catalyst, but it was not very selective for 1,2-PDO.

Combination of physical properties of the as-prepared Ru catalysts in Table 1 reveals that the hydrogenolysis of glycerol is more active on small metal particles. The catalytic performance of the Ru catalysts seems independent of the BET surface area, but partly related to the active metal surface area (Table S1 in the Supplementary material). These results are in good agreement with those reported in published studies

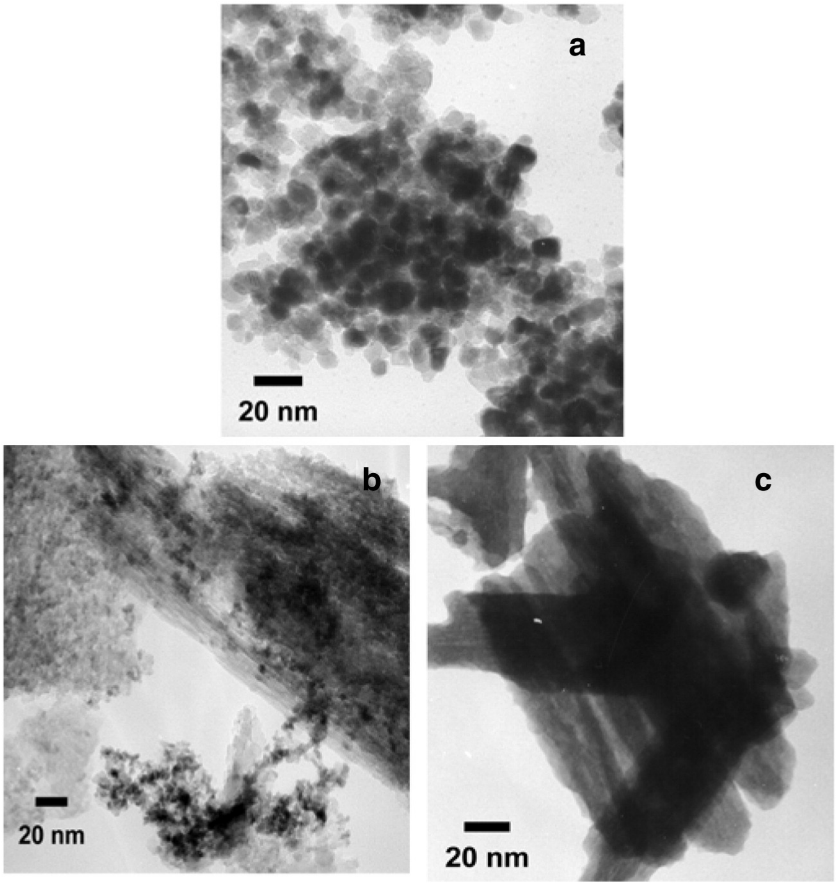

Fig. 3. TEM images of the Ru catalysts: (a) Ru/CeO_2; (b) Ru/MgO; and (c) Ru/La_2O_3.

Table 3
Catalytic performance of the Ru catalysts for the hydrogenolysis of glycerol.[a]

Catalyst	Conversion (%)	Selectivity (%)[b]		
		1,2-PDO	EG	LA
Ru/La_2O_3	31.5	52.8 (16.6)[c]	6.3	8.5
Ru/MgO	60.4	49.7 (30.0)	18.0	21.3
Ru/CeO_2	85.2	62.7 (53.4)	4.2	3.1

[a] Reaction conditions: 3 mL of 20 wt.% glycerol aqueous solution, 180 °C, 5 MPa, 10 h, 50 mg catalyst. EG: ethylene glycol; LA: lactic acid.
[b] Other products: 1-propanol, 2-propanol, ethanol, methanol and methane.
[c] Yield in bracket.

[5–13]. Comparison of the Ru reduction degree, i.e., $Ru^0/(Ru^0 + Ru^{\delta+})$ in Table 1 indicates that the differences in the catalytic performance of the three Ru catalysts are not mainly influenced by the Ru reduction degree. For example, the Ru reduction degree of Ru/MgO was poor than that of Ru/La_2O_3, but the catalytic activity of Ru/MgO was much better. This is possibly because the active metal sites on the catalysts are sufficient to catalyze the reaction even when the reduction degree is low. In fact, increasing the reduction temperature of Ru/MgO to promote the reduction degree is disadvantageous to the hydrogenolysis activity. This phenomenon has been systematically studied in our previous work [13], and it will not be discussed here.

Combination of the base strength distribution of the supports listed in Table 2 shows that the catalyst support with more weak base sites are more active for the hydrogenolysis of glycerol (in the case of Ru/CeO_2). In addition, it seems that the strong base sites in the catalyst support are advantageous to the formation of lactic acid (in the case of Ru/MgO), which is consistent with the results when the glycerol hydrogenolysis reaction is performed over Ru/C in basic aqueous solution [10]. The above-mentioned finding will be useful in selecting other appropriate basic supports for the development of more efficient catalysts. Nevertheless, other factors such as the metal–support interaction may also influence the catalytic performance. Our earlier work has shown that the metal–support interaction will lead to catalyst deactivation [13]. Further research is needed to understand the exact effect between the base sites of the support and the Ru sites, and it will be elucidated in our following work.

3.3. The formation of lactic acid

It is worth noting that an oxidation product lactic acid can be formed under high hydrogen pressure in reductive conditions. The conversion of glycerol to lactic acid can be achieved by hydrothermal decomposition using NaOH as catalyst [27]. Nevertheless, high temperature up to 300 °C is needed to overcome the energy barrier, which is much higher than the reaction temperature (180 °C) in our experiment. In order to examine if the basic oxide supports can catalyze the hydrothermal decomposition of glycerol to lactic acid, we have conducted blank reactions using neat CeO_2, La_2O_3 and MgO under the same reaction conditions in Table 3. However, without Ru metal, almost no reaction occurred, indicating that the basic oxide supports are unable to catalyze the hydrothermal decomposition of glycerol under our reaction conditions. Furthermore, it also suggests that the Ru metal is necessary for the glycerol hydrogenolysis reaction, and lactic acid is not formed directly from glycerol.

In fact, lactic acid and 1,2-PDO can be formed through a same intermediate: 2-hydroxyacrolein [10,28,29]. As we described above, the hydrogenation of 2-hydroxyacrolein over the Ru sites gives 1,2-PDO (see Scheme 1). Of course, 2-hydroxyacrolein can also turn into pyruvaldehyde by keto-enol tautomerism. The combination of experimental results and density functional theory calculations shows that lactic acid can be easily obtained by a Cannizzaro reaction from pyruvaldehyde [28,29]. Based on the known mechanism of Cannizzaro reaction, the reaction pathway for the conversion of 2-hydroxyacrolein to lactic acid is presented in Scheme 2. The hydroxyl ion can be generated from the hydration of the basic oxide supports, which has been proved by the XRD characterization results. This explanation can also account for the high lactic acid selectivity of Ru/MgO, because MgO was all transformed into $Mg(OH)_2$ under hydrothermal condition.

In addition, it should be pointed out that if acidic supports [13] or acidic additives [4–8] are employed, lactic acid will not be formed. This is because the glycerol hydrogenolysis reaction will take place in a different pathway, i.e., the dehydration–hydrogenation mechanism [2,3].

4. Conclusions

Ruthenium supported on basic oxides (Ru/CeO_2, Ru/La_2O_3 and Ru/MgO) have been found to be effective bifunctional catalysts for the hydrogenolysis of glycerol. Ru/CeO_2 exhibited the best performance in terms of the glycerol conversion and of the selectivity to 1,2-PDO. The good performance of Ru/CeO_2 is related to its smaller metal particle size and the weak surface basicity feature of the support. The glycerol hydrogenolysis reaction occurs via a dehydrogenation–dehydration–hydrogenation mechanism. The oxidation product lactic acid is formed by a Cannizzaro reaction from pyruvaldehyde.

Acknowledgments

This work was supported by the National Natural Science Foundation of China (No. 21302237), the Natural Science Foundation Project of CQ CSTC (cstc2011jjA90004), the Opening Project of Key Laboratory of Green Catalysis of Sichuan Institutes of Higher Education (LZJ1104), and the Research Foundation of Chongqing University of Science & Technology (CK2011B13, CK2013Z06).

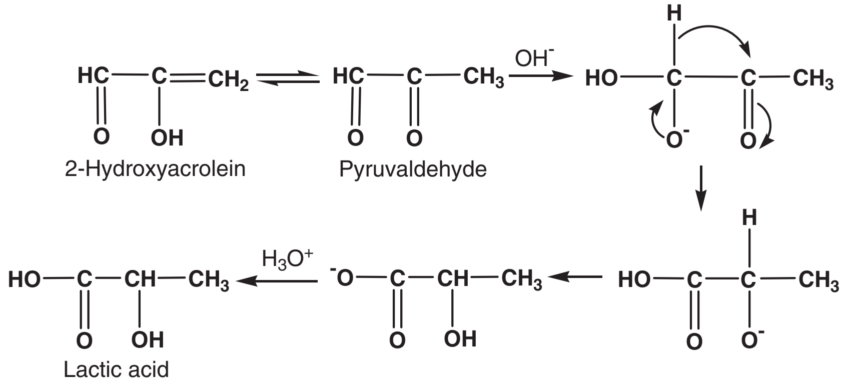

Scheme 2. Conversion of 2-hydroxyacrolein to lactic acid.

Appendix A. Supplementary data

Supplementary data to this article can be found online at http://dx.doi.org/10.1016/j.catcom.2013.11.031.

References

[1] A. Martin, U. Armbruster, I. Gandarias, P.L. Arias, Eur. J. Lipid Sci. Technol. 115 (2013) 9–27.
[2] Y. Nakagawa, K. Tomishige, Catal. Sci. Technol. 1 (2011) 179–190.
[3] J. Feng, M.L. Yuan, H. Chen, X.J. Li, Prog. Chem. 19 (2007) 651–658.
[4] J. Chaminand, L. Djakovitch, P. Gallezot, P. Marion, C. Pinel, C. Rosier, Green Chem. 6 (2004) 359–361.
[5] Y. Kusunoki, T. Miyazawa, K. Kunimori, K. Tomishige, Catal. Commun. 6 (2005) 645–649.
[6] T. Miyazawa, Y. Kusunoki, K. Kunimori, K. Tomishige, J. Catal. 240 (2006) 213–221.
[7] T. Miyazawa, S. Koso, K. Kunimori, K. Tomishige, Appl. Catal. A Gen. 318 (2007) 244–251.
[8] M. Balaraju, V. Rekha, P.S.S. Prasad, B.L.A.P. Devi, R.B.N. Prasad, N. Lingaiah, Appl. Catal. A Gen. 354 (2009) 82–87.
[9] S. Wang, H. Liu, Catal. Lett. 117 (2007) 62–67.
[10] E.P. Maris, R.J. Davis, J. Catal. 249 (2007) 328–337.
[11] E.P. Maris, W.C. Ketchie, M. Murayama, R.J. Davis, J. Catal. 251 (2007) 281–294.
[12] J. Feng, J.B. Wang, Y.F. Zhou, H.Y. Fu, H. Chen, X.J. Li, Chem. Lett. 36 (2007) 1274–1275.
[13] J. Feng, H.Y. Fu, J.B. Wang, R.X. Li, H. Chen, X.J. Li, Catal. Commun. 9 (2008) 1458–1464.
[14] J. Feng, W. Xiong, Y. Jia, J.B. Wang, D.R. Liu, H. Chen, X.J. Li, Chin. J. Catal. 32 (2011) 1545–1549.
[15] J. Feng, B. Xu, W.D. Jiang, W. Xiong, J.B. Wang, Adv. Mater. Res. 549 (2012) 297–300.
[16] J. Feng, B. Xu, D.R. Liu, W. Xiong, J.B. Wang, Adv. Mater. Res. 791–793 (2013) 12–15.
[17] Z.L. Yuan, P. Wu, J. Gao, X.Y. Lu, Z.Y. Hou, X.M. Zheng, Catal. Lett. 130 (2009) 261–265.
[18] S.X. Xia, Z.L. Yuan, L.N. Wang, P. Chen, Z.Y. Hou, Appl. Catal. A Gen. 403 (2011) 173–182.
[19] Z.L. Yuan, L.N. Wang, J.H. Wang, S.X. Xia, P. Chen, Z.Y. Hou, X.M. Zheng, Appl. Catal. B Environ. 101 (2011) 431–440.
[20] S.X. Xia, R.F. Nie, X.Y. Lu, L.N. Wang, P. Chen, Z.Y. Hou, J. Catal. 296 (2012) 1–11.
[21] S. Wang, Y. Li, H. Liu, Acta Chim. Sin. 70 (2012) 1897–1903.
[22] J.I. Take, N. Kikuchi, Y. Yoneda, J. Catal. 21 (1971) 164–170.
[23] P. Käβner, M. Baerns, Appl. Catal. A Gen. 139 (1996) 107–129.
[24] W.Q. Yu, J. Zhao, H. Ma, H. Miao, Q. Song, J. Xu, Appl. Catal. A Gen. 383 (2010) 73–78.
[25] Q.C. Xu, J.D. Lin, X.Z. Fu, D.W. Liao, Catal. Commun. 9 (2008) 1214–1218.
[26] C.M. Hung, Powder Technol. 196 (2009) 56–61.
[27] H. Kishida, F.M. Jin, Z.Y. Zhou, T. Moriya, H. Enomoto, Chem. Lett. 34 (2005) 1560–1561.
[28] J.T. Dam, F. Kapteijn, K. Djanashvili, U. Hanefeld, Catal. Commun. 13 (2011) 1–5.
[29] F. Auneau, C. Michel, F. Delbecq, C. Pinel, P. Sautet, Chem. Eur. J. 17 (2011) 14288–14299.